

Elucidation of the contribution of active site and exosite interactions to affinity and specificity of peptidyl serine protease inhibitors, using non-natural arginine analogs

Masood Hosseini, Longguang Jiang, Hans Peter Sørensen, Jan K. Jensen, Anni Christensen, Sarah Fogh, Cai Yuan, Lisbeth M. Andersen, Mingdong Huang, Peter A. Andreasen, and Knud J. Jensen.

Danish-Chinese Centre for Proteases and Cancer (M.H., L.J., H.P.S., J.K.J., A.C., S.F., C.Y., M.H., P.A.A., K.J.J.); IGM, Faculty of Life Sciences, University of Copenhagen (M.H., K.J.J.); Department of Molecular Biology, Aarhus University (M.H., H.P.S., J.K.J., A.C., S.F., L.M.A., P.A.A.); Fujian Institute of Research on the Structure of Matter, Chinese Academy of Sciences, Fuzhou, China (L.J., C.Y., M.H.)

Running title: Exosite interactions of peptidyl serine protease inhibitors

Corresponding author:

Knud J. Jensen

IGM, Faculty of Life Sciences, University of Copenhagen

Thorvaldsensvej 40, 4 sal

Telephone number: +45 35332430

Fax number: +45 353 32398

e-mail: kjj@life.ku.dk

Number of text pages, 21

Number of tables, 2

Number of figures, 4

References, 36

Abstract words count, 243

Introduction words count, 747

Results words count 2337

Discussion words count, 795

Abbreviations

Alloc: allyloxycarbonyl, Boc: Di-tert-butyl dicarbonate, Cbz: Carboxybenzyl, Dap: L-2,3-Diaminopropionic acid, DIPEA: *N,N*-Diisopropylethylamin, Fmoc: 9H-fluoren-9-ylmethoxycarbonyl, Fmoc-OSu: 9-Fluorenylmethoxycarbonyl-*N*-hydroxysuccinimide, HBTU: *N*-[(1*H*-benzotriazol-1-yl)(dimethylamino)methylene]-*N*-methylmethanaminium hexafluorophosphate *N*-oxide, HBS: Hepes-buffered saline (10 mM Hepes, pH 7.4, 140 mM NaCl), HOBT: *N*-hydroxybenzotriazole, HOAt: 1-hydroxy-7-azabenzotriazole HRMS: High Resolution Mass

Spectrometry. NMP: N-Methyl-2-pyrrolidone, S-2444: pyro-Glu-Gly-Arg-*p*-nitroanilide, TFA: trifluoroacetic acid, uPA: urokinase-type plasminogen activator, wt: wild type.

ABSTRACT

There is increasing interest in developing peptides for pharmacological intervention with pathophysiological functions of serine proteases. From phage-displayed peptide libraries, we previously isolated peptidyl inhibitors of urokinase-type plasminogen activator, a potential target for intervention with cancer invasion. The two peptides, upain-1 (CSWRGLENHRMC) and mupain-1 (CPAYSRYLDC), are competitive inhibitors of human and murine urokinase-type plasminogen activator, respectively. Both have an Arg as the P1 residue, inserting into the S1 pocket in the active site of the enzymes, but their specificity depends to a large extent on interactions outside the enzymes' active sites, so-called exosite interactions. Here we describe upain-2 (CSWRGLENHAAC) and the synthesis of a number of upain-2 and mupain-1 variants in which the P1 Arg was substituted with novel non-natural Arg analogs and achieved considerable improvement in the peptides' affinity to their targets. Using chimeras of human and murine uPA as well as X-ray crystallography, we delineated the relative contribution of the P1 residue and exosite interactions to the affinity and specificity of the inhibitors for their target enzyme. The effect of inserting a particular non-natural amino acid into the P1 position is determined by the fact that changes in interactions of the P1 residue in the S1 pocket leads to changed exosite interactions, and vice versa. These findings are of general interest when considering the affinities and specificities of serine protease inhibitors to be used for pharmacological intervention and could pave the way for potential drug candidates for the treatment of cancer.

Introduction

Recently, peptides have attracted renewed interest as drug candidates. Most often, they display high specificities, comparable to those of monoclonal antibodies, but due to their smaller size, are amenable to chemical modification. They have predictable ADME properties and display a general absence of drug-drug interactions. Although peptides are labile to proteolysis, stable forms can be developed by chemical modification. Moreover, new delivery methods have enabled the formulation of peptide preparations suitable for *in vivo* use (for a review, see (Jorgensen and Nielsen, 2009)).

One important class of potential therapeutic targets is the trypsin family (clan SA) of serine proteases, which has many pathophysiological functions. Therefore, the interest in serine protease inhibitors is increasing (for a review, see (Walker and Lynas, 2001)). Moreover, serine proteases are classical subjects for studies of catalytic and inhibitory mechanisms (for a review, see (Branden and Tooze, 1991)). However, the human genome contains about 200 serine protease genes (for a review, see (Puente, 2008)). Although different serine proteases have different substrate specificities, the catalytic site architectures are highly similar. Achieving sufficient specificity is therefore a challenge of utmost importance when developing serine protease inhibitors. Development of small molecule inhibitors has proved to be a daunting task (for a review, see (Rockway et al., 2002)). To develop inhibitors with a better specificity, a number of peptidyl serine protease inhibitors have recently been isolated by screening phage-displayed peptide libraries, including inhibitors of chymotrypsin (Krook et al., 1998); factor VIIa (Dennis et al., 2000); prostate-specific antigen (Wu et al., 2000); kallikrein-2 (Heinis et al., 2009; Hekim et al., 2006); mannose-binding lectin-associated serine protease-1 and -2 (Kocsis et al., 2010); furins (Hajdin et al., 2010); and isoforms of trypsin (Wu et al., 2010).

One example of a serine protease that is a potential drug target is urokinase-type plasminogen activator (uPA), which catalyzes the conversion of plasminogen to the active protease plasmin. Plasmin in turn catalyzes directly the degradation of extracellular matrix proteins. Upregulation of uPA is implicated in tissue remodeling in several pathological conditions. In particular, uPA is central to the invasive capacity of malignant tumors (for a review, see (Andreasen et al., 2000)). We previously isolated two peptides, one (upain-1, CSWRGLENHRMC) being an inhibitor of human uPA (Hansen et al., 2005), the other (mupain-1, CPAYSRYLDC) being an inhibitor of murine uPA

(Andersen et al., 2008). Both are constrained in a circular form by a disulfide bridge. Both are highly specific for the target enzyme against which they were selected. Thus, upain-1 binds about 500-fold better to human uPA than to murine uPA, while mupain-1 binds more than 2000-fold better to murine uPA than to human uPA. Both bind very selectively to uPA as compared to other serine proteases from the same species (Andersen et al., 2008; Hansen et al., 2005). Analysis of the inhibitory mechanism showed that both upain-1 and mupain-1 are competitive inhibitors of their target enzymes (Andersen et al., 2008; Hansen et al., 2005). Site-directed mutagenesis (Andersen et al., 2008; Hansen et al., 2005) and X-ray crystal structure analysis (Zhao et al., 2007) showed that Arg4 of upain-1 and Arg6 of mupain-1 are the P1¹ residues of these peptides, *i.e.*, inserts into the enzymes' S1 or specificity pocket, the primary interaction site between substrate and enzyme. In the case of upain-1, X-ray crystal structure analysis showed that the side-chain of the peptide's Glu7 blocks the enzyme's oxyanion hole (Zhao et al., 2007). Upain-1 and mupain-1 thus directly occupy the structures of the active sites which are essential for the catalytic machinery for peptide bond hydrolysis (for a review, see (Hedstrom, 2002)). However, the great specificity of both peptides is achieved by a large interaction area, involving not only the active sites, but also surface-exposed loops specific for individual proteases, *i.e.*, exosite interactions.

Upain-1 inhibits human uPA with a K_i of around 40 μM at 37°C. Mupain-1 has a considerably higher, although still not quite satisfactory affinity to murine uPA, with a K_i of around 0.4 μM at 37°C. In an effort to engineer the peptides to higher affinity while maintaining specificity and to understand enzyme-inhibitor interactions, we have first made two amino acid substitutions in upain-1 to obtain upain-2 and, second, substituted the P1 L-Arg residues in mupain-1 and upain-2 with a variety of novel non-natural arginine analogs. By testing different P1 residues in uPA variants with different S1 pockets and different surface loops, we have evaluated the importance of S1 pocket interactions versus exosite interactions for the affinity and specificity of the peptides.

Materials and methods

General. Chemicals were purchased from Sigma-Aldrich, Iris Biotech GmbH, Rapp Polymere GmbH and used without further purification unless otherwise stated. Fmoc-HArg(Pbf)-OH, Fmoc-L-Dap-N-amidine(N,N'-di-Boc)-OH, Fmoc-L-NorArg(N,N'-di-Boc)-OH, Fmoc-Citrulline-OH, Fmoc-L-4-guanidino-phenylalanine(N,N'-di-Boc)-OH, Fmoc-L-2,3-diaminopropionic acid-OH, Fmoc-L-BisHomoarginine(Pmc)-OH, Fmoc-D-Arg(Pbf)-OH, Fmoc-L-Ala-4-Piperidyl(Alloc)-OH, Fmoc-L-3Pal-OH and Fmoc-L-canavanine(Boc)-OH were commercially available. 4-(2,3-Bis(tert-butoxycarbonyl)guanidino)benzoic acid was synthesized according to a previously published procedure (Kayser et al., 2007). NMR was performed using a Bruker Avance 300 spectrometer. Analytical HPLC was performed on a Dionex UltiMate 3000, using a Phenomenex Gemini 110 Å C18 column (3 μm, 4.6 × 50 mm) with a flow rate of 1.0 ml/min and a linear gradient going from 95% H₂O/5% acetonitrile with 0.1% HCOOH to 100% acetonitrile with 0.1% HCOOH over 10 min. Preparative HPLC was performed using a Dionex UltiMate 3000, equipped with a Phenomenex Gemini-NX C18 110 Å column running at a flow rate of 10.0 ml/min and a linear gradient going from 95% H₂O/5% acetonitrile with 0.1% TFA to 100% acetonitrile with 0.1% TFA over 30 min. High resolution mass spectra were obtained on a Micromass LCT high resolution time-of-flight instrument by direct injection. Ionization was performed in positive electrospray mode.

General methods for solid-phase peptide synthesis. Peptide synthesis was performed using N^α-Fmoc protected amino acids and a HBTU/HOBt activation protocol using a Tentagel resin with Rink amide linker (0.23 mmol/g); HBTU (3.8 Eq), HOBt/HOAt (4:1, 4 Eq), Fmoc-AA-OH (4 Eq), DIPEA (7.2 Eq) in NMP. Preactivation for 5 min and single couplings for 90 min. Fmoc deprotection was performed using piperidine/NMP (1:4) for 2+15 min. Peptides with Alloc protected amino acids were deprotected to a free amine by treating the fully protected and N-acetylated peptides with a mixture of Pd(PPh₃)₄ (0.05 Eq) and Me₂NH-BH₃ (0.2 Eq) in degassed CH₂Cl₂ (30 min) and washed with NMP (5 x). The peptides were then treated with N,N'-di-Boc-1H-pyrazole-1-carboxamide (5 Eq) in NMP overnight. Following peptide assembly, the resins were washed extensively with NMP and CH₂Cl₂, before peptide release with TFA/H₂O/triethylsilane (95:2.5:2.5). Peptide release normally proceeded for 2 h before the TFA-peptide mixture was collected by filtration. The resin was

additionally washed with TFA (2x) and the TFA mixtures were pooled. TFA was removed under a stream of nitrogen and the peptide was precipitated with diethyl ether. The synthesized peptides were dissolved in a minimum amount of H₂O/acetonitrile (2:1) before being purified by preparative HPLC. The purified peptides were dissolved in H₂O/acetonitrile (2:1) to a final concentration of 1 mM. The solution was brought to pH 7.5-8 with NH₃ in methanol. The peptides were oxidized to form disulfide bridges, either by addition of 1.2 Eq of H₂O₂ (30-60 min) or by bubbling atmospheric air through the solution (1-3 days). The use of H₂O₂ is only applicable in peptides without a methionine (upain-2 and mupain-1 variants). The oxidization was stopped with the addition of acetic acid (0.1 ml) followed by evaporation and HPLC purification.

Synthesis of Fmoc-Dap(4-(2,3-bis(Boc)guanidino)benzoate)-OH (protected form of 11).

PyBOP (Benzotriazol-1-yloxy-tripyrrolidinophosphonium hexafluorophosphate) (1040 mg, 2.0 mmol) and DIPEA (0.35 ml, 2.0 mmol) were added to a solution of 4-(2,3-bis(tert-butoxycarbonyl)guanidino)benzoic acid (800 mg, 2.1 mmol) in CH₂Cl₂ (5 ml). The mixture was stirred for 10 min at room temperature and transferred to a solution of Fmoc-Dap-OH (326 mg, 1.0 mmol) in CH₂Cl₂ (6 ml). DIPEA (0.35 ml, 2.0 mmol) was added and the mixture stirred for 18 h at room temperature. The mixture was evaporated and purified by column chromatography with ethyl acetate/acetic acid (99:1) to afford the product as a yellow oil (421 mg, 61%).

¹H NMR (300 MHz, CDCl₃) δ ppm 7.78-7.48 (m, 10H), 7.38-7.20 (m, 4H), 4.45-4.05 (m, 3H), 3.88-3.63 (m, 2H), 1.50-1.62 (bs, 9H). ¹³C (75 MHz, CDCl₃) δ ppm 172.2, 168.6, 156.9, 153.6, 143.7, 143.6, 141.2, 141.1, 139.8, 129.4, 128.7, 128.2, 127.6, 127.0, 125.1, 122.2, 120.9, 119.8, 67.3, 55.1, 46.9, 28.0. HRMS (ES) exact mass calculated for C₂₆H₂₆N₅O₅ (M+H-2Boc) 488.1934 found 488.1938.

Synthesis of Fmoc-4-(N,N'-Di-Cbz-guanidine)-Cha-OH (protected form of 15). To a degassed (Argon) solution of Boc-Phe(4-NO₂)-OH (1 g, 3.22 mmol) in acetic acid (3 ml) and methanol (3 ml) was added PtO₂ (500 mg) and H₂ was bubbled through the mixture until completion of the reaction as determined by HPLC (9 h). The mixture was co-evaporated several times with toluene. The green solid was dissolved in dimethylformamide (5 ml) and to this mixture was added N,N'-bis(benzyloxycarbonyl)-1H-pyrazole-1-carboximidine (1250 mg, 3.30 mmol) and Et₃N (0.45 ml, 3.23 mmol) and stirred overnight. The mixture was evaporated and ethyl acetate (30 ml) was added

and extracted with aqueous NaHCO₃ (10%, 3 x 20 ml). The aqueous solution was acidified to pH 2-3 with aqueous HCl (37 %) and extracted with CH₂Cl₂ (3 x 30 ml) and evaporated. TFA/CH₂Cl₂ (1:1, 10 ml) was added and the mixture was stirred for 15 min, then evaporated to an oil and left on high vacuum overnight. The solid was dissolved in H₂O/dioxane (1:2, 60 ml). To this was added Fmoc-OSu (1.20 g, 3.56 mmol) and NaHCO₃ (550 mg, 6.55 mmol) and the mixture left stirring overnight. The mixture was evaporated, re-dissolved in acetic acid (5 ml) and celite (3 g) was added. The slurry was evaporated and purified by silica-gel column chromatography with ethyl acetate/heptane/acetic acid (50:50:1) providing 813 mg (35%). The product is presumably a cis/trans isomer (Rao et al., 1991). ¹H NMR (300 MHz, CDCl₃) δ ppm 7.55-7.63 (d, *J* = 7.3 Hz, 2H), 7.52-7.61 (m, 2H), 7.32-7.45 (m, 10H), 5.16-5.05 (m, 5H), 4.31 - 4.05 (m, 4H), 2.59 (s, 0.2H), 2.30 (s, 0.8H), 2.05-1.02 (m, 8H). ¹³C (75 MHz, CDCl₃) δ ppm 176.6, 176.5, 163.8, 156.1, 155.2, 155.1, 154.0, 153.8, 148.5, 143.9, 143.8, 143.6, 141.3, 137.8, 136.8, 136.8, 134.6, 134.5, 134.5, 125.0, 120.0, 68.4, 68.1, 67.1, 51.7, 49.5, 47.1, 46.3, 38.6, 32.4, 32.2, 30.5, 29.2, 29.1, 28.1, 26.9, 21.4. HRMS (ES) exact mass calculated for C₄₁H₄₃N₄O₈ (M+H) 719.3081 found 719.3044.

Synthesis of Fmoc-L-3-(N-amidino-3-piperidyl)alanine-OH (Precursor for 17). Fmoc-L-3Pal-OH (700 mg, 1.8 mmol) was dissolved in acetic acid (10 ml) in a round-bottomed flask and PtO₂ (500 mg) was added. The solution was degassed and the flask was connected a hydrogen balloon and the mixture was left stirring overnight. The mixture was filtered and evaporated to a clear oil. The oil was furthermore evaporated with toluene (3 x 30 ml) to remove acetic acid residues. The oil was dissolved in acetonitrile/H₂O (2:1, 50 ml) and DIPEA (0.15 ml, 0.9 mmol) and Alloc₂O (285 mg, 2.0 mmol) was added. The mixture was stirred at room temperature until the completion of the reaction as determined by HPLC (1 h). The mixture was evaporated and purified by column chromatography with ethyl acetate/heptane/acetic acid (1:1:0.02) to afford the product as a white foam (650 mg, 75%). The product is presumably a mixture of diastereomers (Hartung et al., 2005). ¹H (300 MHz, CDCl₃) δ ppm 8.02 (s, 1H), 7.76 (d, *J* = 7.5 Hz, 1H), 7.60 (d, *J* = 6.3 Hz, 1H), 7.40 (t, *J* = 7.3 Hz, 1H), 7.35 - 7.24 (m, 1H), 5.93 (dd, *J* = 16.3, 9.6 Hz, 1H), 5.34 - 5.03 (m, 1H), 4.71 - 4.32 (m, 3H), 4.23 (t, *J* = 7.0 Hz, 1H), 4.03 - 3.75 (m, 1H), 3.12 - 2.46 (m, 1H), 1.97 - 1.04 (m, 4H). ¹³C (75 MHz, CDCl₃) δ ppm 176.09, 156.52, 156.24, 155.50, 143.95, 143.74, 141.37, 133.00, 127.80, 127.16, 126.13, 125.22, 120.06,

117.60, 116.49, 67.63, 67.20, 66.38, 51.89, 51.64, 49.78, 49.03, 47.20, 44.72, 36.04, 32.41, 30.62, 29.87, 24.43. MS (ES) calculated for C₂₇H₃₁N₂O₆ (M+H) 479.2, found 479.1.

Synthesis of Fmoc-3-(N,N'-di-Boc-guanidine)-Tyr-OH (protected form of 14). A solution of H-Tyr(3-NO₂)-OH (1000 mg, 4.42 mmol) in dioxane/H₂O (2:1, 20 ml), NaHCO₃ (1280 mg, 15.2 mmol) and Fmoc-OSu (1710 mg, 5.1 mmol) in a round-bottomed flask was stirred overnight at room temperature. After degassing the solution, Pd/C was added and a hydrogen balloon was connected. The mixture was stirred for 2 h, filtered (celite) and evaporated. To this solid was added CH₂Cl₂ (5 ml) which formed a suspension and N,N'-di-Boc-1H-pyrazole-1-carboxamide (1530 mg, 4.94 mmol) was added and the mixture left stirring overnight. The mixture was evaporated with celite and purified by column chromatography ethyl acetate/heptane/acetic acid (1:1:0.01) providing 1980 mg (68%).

¹H NMR (300 MHz, CDCl₃) δ ppm 10.1 (bs, 4H), 7.82-7.13 (m, 11H), 7.04-6.77 (m, 3H), 5.48 (d, J = 7.7 Hz, 1H), 4.53-4.12 (m, 4H), 3.32-2.95 (m, 2H), 1.61-1.40 (bs, 18H). ¹³C (75 MHz, CDCl₃) δ ppm 174.9, 160.9, 155.8, 153.1, 153.0, 148.4, 143.8, 143.7, 141.3, 141.2, 132.9, 129.0, 128.7, 128.2, 127.7, 127.1, 125.3, 125.2, 125.1, 124.7, 124.6, 121.0, 119.9, 84.7, 80.9, 67.1, 54.9, 47.1, 36.7, 28.1, 21.4. HRMS (ES) exact mass calculated for C₂₅H₂₅N₄O₅ (M+H-2Boc) 461.1825, found 461.1831.

Synthesis of Fmoc-L-Phg-3-(N,N'-di-Boc-guanidine)-OH (protected form of 13). L-Phenylglycine (5 g, 33 mmol) was dissolved in 97% H₂SO₄ (12 ml) and cooled to 0°C. To this solution was added 37% HNO₃ (1.5 ml, 36 mmol) drop wise. The mixture was stirred at 0°C for 1 h and neutralized with 25% NH₄OH/H₂O (20 ml). When reaching pH 7 a yellow precipitate formed which was filtered off and washed with cold deionized H₂O. The precipitate was recrystallized with H₂O to afford 3-nitrophenylglycine as a white solid (Sassatelli et al., 2006). The solids were dissolved in H₂O/dioxane (2:3, 100 ml). Fmoc-OSu (7.0 g, 21 mmol) and Na₂CO₃ (3.6 g, 34 mmol) were added. The mixture was stirred at room temperature (18 h) and acidified to pH 2 by 37% HCl. To this was added H₂O (150 ml) and the mixture was extracted with ethyl acetate (100 ml). The organic phase was washed with H₂O (100 ml) and brine (100 ml) and evaporated. Acetic acid (50 ml) and Pd/C (300 mg) was added and the mixture was left stirring under 1 atm H₂ for 12 h. The mixture was filtered with celite and evaporated to a yellow oil (8.72 g). To 450 mg of this oil in dimethylformamide (10 ml) was added N,N'-di-Boc-1H-pyrazole-1-carboxamide (400 mg, 1.3 mmol) and triethylamine (0.35 ml, 2.5

mmol) and the mixture was stirred for 3 h at room temperature. The mixture was evaporated and purified by column chromatography heptane/ethyl acetate/acetic acid (40:40:1) to give the product (620 mg, 85%) as a yellow foam. ^1H NMR (300 MHz, CDCl_3) δ ppm 1.34 - 1.63 (m, 18 H) 4.07 - 4.55 (m, 3 H) 4.94 - 5.42 (m, 1 H) 6.00 - 6.43 (m, 1 H) 7.03 - 8.10 (m, 15 H) ^{13}C (75 MHz, CDCl_3) δ ppm 28.1, 31.2, 47.2, 58.0, 67.2, 105.6, 119.9, 122.1, 123.3, 123.7, 124.3, 125.2, 127.1, 127.7, 128.3, 129.1, 129.5, 133.0, 136.5, 137.9, 138.3, 141.3, 143.9, 153.2, 154.2, 155.5, 160.4, 173.1, HRMS (ES) exact mass calculated for $\text{C}_{34}\text{H}_{39}\text{N}_4\text{O}_8$ 631.2768, found 631.2767.

Synthesis of (S)-2-acetamido-6-guanidinohexanamide. To a solution of Fmoc-Lys(Alloc)-OH (181 mg, 0.4 mmol) in NMP (2 ml) was added HBTU (140 mg, 0.37 mmol) and DIPEA (0.12 ml, 0.72 mmol) and the mixture was added to Tentagel resin (417 mg, 0.1 mmol). The mixture was carefully shaken (2 h) and washed several times with NMP. The resin was treated with piperidine/NMP (1:4, 2+15 min) and washed several times with NMP and CH_2Cl_2 and treated with $\text{Ac}_2\text{O}/\text{CH}_2\text{Cl}_2$ (1:2, 2 x 7 min). To the resin was added degassed CH_2Cl_2 and $\text{Pd}(\text{PPh}_3)_4$ (30 mg, 0.026 mmol) and $\text{BH}_3\text{-HN}(\text{CH}_3)_2$ complex (25 mg, 0.45 mmol). The mixture was shaken for 30 min and washed several times with NMP. To the resin was added N,N'-di-Boc-1H-pyrazole-1-carboxamidine (310 mg, 1.0 mmol) in NMP (2 ml) and the mixture was shaken overnight at room temperature. The resin was treated with TFA/triethylsilane/ H_2O (95:2.5:2.5, 2 h). The mixture was evaporated under a stream of N_2 and the product was purified by preparative HPLC to provide 14 mg (64%). ^1H NMR (300 MHz, D_2O) δ 4.25 (dd, $J = 8.9, 5.4$ Hz, 1H), 3.20 (t, $J = 6.9$ Hz, 2H), 1.92 - 1.69 (m, 2H), 1.61 (dd, $J = 14.4, 6.9$ Hz, 2H), 1.52 - 1.35 (m, 2H). ^{13}C NMR (75 MHz, D_2O) δ ppm 156.7, 53.4, 40.8, 30.4, 27.3, 22.1, 21.6. HRMS (ES) exact mass calculated for $\text{C}_9\text{H}_{20}\text{N}_5\text{O}_2$ (M+H) 230.1617, found 230.1609.

Synthesis of (S)-2-acetamido-3-(4-guanidinophenyl)propanamide. HBTU (140 mg, 0.37 mmol) and DIPEA (0.12 ml, 0.72 mmol) was added to a solution of Fmoc-4-guanidinophenylalanine(N,N'-di-Boc)-OH (258 mg, 0.4 mmol) in NMP (2 ml) and the mixture was added to Tentagel resin (417 mg, 0.1 mmol). The mixture was carefully shaken (2 h) and washed several times with NMP. To the resin was added piperidine/NMP (1:4, 2+15 min) and the mixture washed several times with NMP and CH_2Cl_2 , subsequently the resin was treated with $\text{Ac}_2\text{O}/\text{CH}_2\text{Cl}_2$ (1:2, 2 x 7 min) and washed several times with CH_2Cl_2 . The resin was then treated with TFA/triethylsilane/ H_2O

(95:2.5:2.5, 2h). The mixture was evaporated under a N₂ flow and the product was purified by preparative HPLC (11 mg, 44%).

¹H NMR (300 MHz, D₂O) δ 7.57 - 7.25 (m, 4H), 4.66 - 4.54 (m, 1H), 3.25 (dd, *J* = 14.0, 6.0 Hz, 1H), 3.03 (dd, *J* = 13.9, 9.3 Hz, 1H), 1.96 (s, 3H). ¹³C NMR (75 MHz, D₂O) δ 137.5, 136.1, 132.5, 130.3, 130.1, 128.2, 125.5, 122.6, 118.7, 118.2, 117.8, 114.0, 54.1, 36.1, 21.1. HRMS (ES) exact mass calculated for C₁₂H₁₈N₅O₂ (M+H) 264.1461, found 264.1476.

Synthesis of (S)-2-acetamido-3-(1-carbamimidoylpiperidin-4-yl)propanamide. To a solution of Fmoc-L-Ala(4-Pip(Alloc))-OH (191 mg, 0.4 mmol) in NMP (2 ml) was added HBTU (140 mg, 0.37 mmol) and DIPEA (0.12 ml, 0.72 mmol) and the mixture was added to a Tentagel resin (417 mg, 0.1 mmol). The mixture was carefully shaken (2 h) and washed several times with NMP. The resin was treated with piperidine/NMP (1:4, 2+15 min) and the mixture washed several times with NMP and CH₂Cl₂, subsequently the resin was treated with Ac₂O/CH₂Cl₂ (1:2, 2 x 7 min) and washed several times with CH₂Cl₂. To the resin was added degassed CH₂Cl₂, BH₃·HN(CH₃)₂ complex (25 mg, 0.45 mmol) and Pd(PPh₃)₄ (30 mg, 0.026 mmol). The mixture was shaken for 30 min and washed several times with NMP. N,N'-Di-Boc-1H-pyrazole-1-carboxamide (310 mg, 1.0 mmol) in NMP (2 ml) was added and the mixture was shaken overnight at room temperature. The resin was treated with TFA/triethylsilane/H₂O (95:2.5:2.5, 2 h). The mixture was evaporated under a N₂ flow and the product was purified by preparative HPLC (10 mg, 39%). ¹H NMR (300 MHz, D₂O) δ 4.22 (t, *J* = 7.3 Hz, 1H), 3.70 (d, *J* = 13.8 Hz, 2H), 2.95 (dd, *J* = 23.7, 10.9 Hz, 2H), 1.94 (s, 3H), 1.76 - 1.52 (m, 5H), 1.29 - 1.02 (m, 2H). ¹³C NMR (75 MHz, D₂O) δ ppm 177.3, 174.4, 155.6, 51.1, 45.8, 45.7, 37.0, 31.4, 30.9, 29.7, 21.6. HRMS (ES) exact mass calculated for C₁₁H₂₂N₅O₂ (M+H) 256.1774, found 256.1782.

Recombinant uPA expression and purification. Two-chain human uPA, originating from urine, was purchased from Wakamoto Pharmaceutical Company, Tokyo, Japan or Prospec, Rehovot, Israel. Human uPA concentrations were determined from the absorbance at 280 nm, using an extinction coefficient of 1.36 ml mg⁻¹ cm⁻¹ and an *M_r* value of 54,000. Two-chain murine uPA was purchased from Molecular Innovations (Novi, MI, USA). Wt and mutant recombinant human and murine uPA were expressed in, and in some cases purified from, HEK293T cells transfected with the corresponding cDNAs in pcDNA3.1 (Andersen et al., 2008; Petersen et al., 2001).

When the cells were cultured without addition of protease inhibitors able to inhibit the conversion of single-chain pro-uPA to active two-chain uPA, like aprotinin, approximately 50% of the uPA in the conditioned medium and the purified preparations were in the active form and could thus be used directly for enzymatic assays. Three mutant sets of mutant cDNAs were cloned into pcDNA3.1 and used to obtain the corresponding proteins. First, murinized human uPA variants, harbouring the point mutations H99Y², Q192K, or H99Y-Q192K, were those described previously (Andersen et al., 2008). Second, humanized murine uPA variants, in which the point mutation K192Q was introduced into murine uPA or in which the human 37, 60, and 99 loops were grafted onto murine uPA, were constructed by standard cloning procedures and customized DNA synthesis (Genscript). More specifically, the murine uPA variant with human 37, 60, and 99 loops harbours the mutations Q35R, K36R, N37H, K37aR, Q60aD, L60bY, N63D and Y99H. Third, cDNA corresponding to chimeras of human and mouse uPA, in which position 22-120 or 121-250 of human uPA replaced the corresponding residues in a murine uPA background, were synthesized by Genscript. Conditioned media from the HEK293T transfectants were used directly for the analysis of kinetic parameters and inhibition constants for the various uPA variants. In a few cases (wt human uPA, wt murine uPA, murine uPA with human residues 16 - 120, and murine uPA with human residues 121 - 250), it was shown that the same kinetic parameters and inhibition constants were obtained with conditioned media and purified preparations.

The cloning strategy and the production of recombinant uPA catalytic domain (residues 159-411) to be used for crystallisation was described previously (Zhao et al., 2007). Basically, the recombinant uPA catalytic domain was secreted from a stable *Pichia pastoris* strain (X-33) after induction by methanol and captured by a cation exchange column. The protein was further purified on a gel filtration column (Superdex 75 HR 10/30 column from GE Health Care) equilibrated with 20 mM sodium phosphate, pH 6.5, 150 mM NaCl. The protein was eluted as a single peak under these conditions, with a retention time of approximately 13.6 ml. The recombinant uPA catalytic domain expressed this way is an active protease with an activity comparable to full-length two-chain uPA (Zhao et al., 2007). The protein was dialysed in 20 mM potassium phosphate, pH 6.5 overnight and

concentrated to 10 mg/ml, using stirred ultrafiltration cells (Millipore and Amicon Bioseparations, Model-5124), prior to protein crystallization.

Determination of K_M values for uPA-catalysed hydrolysis of S-2444. To determine the K_M and maximal velocity (V_{max}) values for the uPA-catalysed hydrolysis of the chromogenic substrate S-2444 (pyro-Glu-Gly-Arg-*p*-nitroanilide), a 200 μ L 2-fold dilution series of the substrate S-2444 (0 - 4 mM) in a buffer of 10 mM HEPES, pH 7.4, 140 mM NaCl (HEPES-buffered saline, HBS), with 0.1% BSA, was incubated 2 min at 37°C, prior to the addition of a fixed concentration of uPA (4 nM final concentration). The initial reaction velocities (V_i), monitored as the changes in absorbance at 405 nm, were plotted against the initial substrate concentration ($[S]$) and non-linear regression analysis was used to determine the K_M according to equation 1:

$$V_i = V_{max} [S] / ([S] + K_M) \quad (\text{Eq. 1})$$

The K_M values for all the uPA variants employed in the present study are listed in the supplementary material (Supplemental Table 1).

Determination of K_i values for the inhibition of uPA variants by upain-2 and mupain-1 variants. The concentrations of the peptide variants were determined by measurements of OD₂₈₀ and the use of sequence-derived extinction coefficients provided by the ProtParam tool provided by the ExPASy server (located at <http://www.expasy.org>). For routine determination of K_i values for the inhibition of the various uPA variants under steady state inhibition conditions, a fixed concentration of purified uPA or uPA-containing conditioned media from transfected cells (2 nM uPA as the final concentration) was pre-incubated in a 200 μ L HBS with 0.1% BSA at 37°C, with various concentrations of upain-2 or mupain-1 variant peptides (0 - 400 μ M) for 15 min prior to the addition of the chromogenic substrate S-2444 in concentrations approximately equal to the K_M value for each particular variants. The initial reaction velocities were monitored at an absorbance of 405 nm. The inhibition constants (K_i) were subsequently determined from the non-linear regression analyses of plots for V_i/V_o versus $[I]_0$ using Equation 2, derived under assumption of competitive inhibition:

$$V_i/V_o = (K_i \times (K_M + [S]_0)) / ((K_i \times [S]_0) + (K_M \times (K_i + [I]_0))) \quad (\text{Eq. 2})$$

where V_i and V_o are the reaction velocities in the presence and absence of inhibitor, respectively; $[S]_0$ and $[I]_0$ are the substrate and inhibitor concentrations, respectively; K_M is K_M for the uPA catalysed

hydrolysis of S-2444. In Equation 2, it is assumed that $[S]_{\text{free}} \approx [S]_0$ and $[I]_{\text{free}} \approx [I]_0$. These conditions were fulfilled as less than 10% of the substrate was converted to product in the assays and as the assay typically contained a final concentration of uPA variant of 2 nM and inhibitor concentrations in the μM range.

In cases, in which we observed no measurable inhibition (*i.e.*, < 10%) at 400 μM , the maximal inhibitor concentration used, the accuracy of the assay allowed us to conclude that the K_i value was more than 1000 μM (indicated as “> 1000 μM ” in the tables). In other cases, in which we did observe a measurable inhibition at 400 μM , we were still unable to accurately determine K_i values above 500 μM (indicated as “> 500 μM ” in the tables).

The validity of performing the K_i determinations with uPA-containing conditioned media from transfected cells was verified by controls in which the determinations were performed with conditioned media as well as with purified preparations. These controls were performed with murine uPA wt, human uPA wt, human uPA Q192K, and murine uPA, human residues 16 - 120, obtaining indistinguishable values with the types of samples.

X-ray crystal structure analysis. The crystallization trials were carried out using the method of sitting drop vapour diffusion. The crystals of uPA catalytic domain were obtained by equilibrating against a reservoir solution containing 2.0 M ammonium sulfate, 50 mM sodium citrate, pH 4.6, 5% PEG 400 at room temperature. The crystals appeared in about three days. For the uPA-**upain-2-13** complex, the crystals of uPA were then soaked for two weeks in crystallisation mother liquid containing 1 mM **upain-2-13**. Prior to X-ray data collection, the crystals were soaked for 5 min in a cryoprotectant solution (2.0 M ammonium sulfate, 5% polyethylene glycol 400, 100 mM Tris-HCl, pH 7.4, 20% glycerol).

X-ray diffraction data of the crystals were collected at the BL17U1 beamline, Shanghai Synchrotron Radiation Facility. All diffraction data were indexed and integrated by HKL2000 programme package (Otwinowski and Minor, 1997) .

The crystal structure of the uPA-**upain-2-13** complex was solved by molecular replacement with the CCP4 programme package (Collaborative Computational Project 1994), using the structure of

the uPA catalytic domain (PDB file 2NWN) (Zhao et al., 2007) as the search model. The electron density for the peptide was clearly visible in the uPA active site and was modelled based on the Fo-Fc difference map. The structure was refined with the CCP4 programme package (Collaborative Computational Project 1994) and manually adjusted by the molecular graphics program COOT (Emsley and Cowtan, 2004), iteratively until the convergence of the refinement. Solvent molecules were added using a Fo-Fc Fourier difference map at 2.5 sigma in the final refinement step. The final structures were analysed by software Pymol (DeLano, 2002).

Results

Non-natural arginine analogs. The P1 Arg residue in mupain-1 was systematically substituted with a series of Arg analogs. Concerning upain-1, the novel P1 residues were substituted into the modified sequence CSWRGLENHAAC (upain-2)³. This modification was chosen, as the cyclization step could be performed much faster when Arg10 of upain-1 (CSWRGLENHRMC) was replaced with Ala and, secondly, H₂O₂ could be used as an oxidant when Met11 was absent. As predicted from our previous report (Hansen et al., 2005), the modified sequence bound to human uPA with a K_i indistinguishable from that of the original peptide: $35 \pm 8 \mu\text{M}$ (n=5) for the modified sequence versus $30 \pm 1 \mu\text{M}$ (n=3) for the original sequence. When planning which arginine analogs to test as P1 residue in upain-2 and mupain-1, we considered varying several parameters, all expected to affect the interaction of the P1 residue with the S1 pocket (Table 1).

1. The chirality of the P1 residue was tested by substituting L-Arg (**1**) with D-Arg (**3**).
2. The length of the aliphatic side-chain was tested by substituting arginine with homologs containing 1 to 5 methylene groups between the α -carbon and the guanidino group (**4-7**). Besides determining how far the guanidino moiety can insert into the S1 pocket, the spacer length could also have an effect on the binding entropy and the strength of hydrophobic interactions.
3. The exact nature of the basic group could be tested by replacing the guanidino group of L-Arg with a urea moiety ($\text{pK}_a = 12$), an amino group ($\text{pK}_a = 10$), or a guanidino-oxo group ($\text{pK}_a = 7$) (Boyar and Marsh, 1982).
4. The structure of the carbon skeleton between the α -carbon and the basic group was varied by introducing aliphatic or aromatic rings (**11-14**). Aromatic rings would also be spatially more demanding and restrict the conformational orientations and potentially mimic already reported small-molecule inhibitors. They would also result in a lower pK_a value of the guanidino moiety. Cyclic aliphatic groups would restrict the conformational orientations (**15-17**).

While a variety of arginine analogs are commercially available, more arginine analogs had to be synthesized *de novo* (Figure 1) in order to complete the planned scan of the P1 position (Table 1). We

here designed and synthesized the following novel arginine analogs: 4-guanidino-L-cyclohexylalanine (**15**); 3-guanidino-L-tyrosine (**14**); 3-guanidino-L-phenylglycine (**13**); (S)-2-amino-3-(4-guanidinobenzamido)propanoic acid (**11**); L-3-(N-amidino-3-piperidyl)alanine (**17**).

With the *de novo* synthesized arginine analogs and the commercially available analogs at hand for insertion into the P1 position, linear forms of the peptides were assembled by solid-phase peptide synthesis. The peptides were obtained as the N-terminally acetylated and C-terminally amidated forms and were cyclized by disulfide bridge formation.

Effects of P1 substitutions on the inhibition of human uPA by upain-2 and of murine uPA by mupain-1. We investigated the effect of substituting the different analogs into the P1 position of upain-2 or mupain-1 on their ability to inhibit human or murine uPA (Table 1). The binding of the peptide to their targets was critically dependent on the side chain of the P1 residue, as substitution of P1 Arg with Ala (**2**) abolished all inhibitory activity.

Substitution of P1 Arg in upain-2 with a number of L-Arg analogs with linear aliphatic side chains (**3 - 10**) in almost all cases resulted in a strong loss of activity. Neither a change in chirality, variation in the chain length, nor exchange of the guanidino group with a urea moiety, an amino group, or a guanidino-oxo group was accepted. The only exception was substitution with L-homo-arginine (**6**), which resulted in a slight improvement of affinity. Moreover, substitution with aromatic (**11 - 14**) or aliphatic ring structures (**15 - 17**) always resulted in a strong loss of inhibitory activity.

Similarly to upain-2, substitution of the P1 Arg in mupain-1 with L-Arg analogs containing linear aliphatic side chains (**3 - 10**) in all cases resulted in loss of inhibitory activity, with an increase in K_i of between 5 and > 2000-fold. The response to substitution with L-Arg analogues with aromatic ring structures (**11 - 14**) was more varied, as the substitution with the Phe analog **12** resulted in a slight increase in affinity, while other substitutions resulted in a strong loss of affinity. Moreover, inhibition of murine uPA could still be achieved with L-Arg analogs with aliphatic ring structures (**15- 17**). In fact, substitution with the amidino compound **16** resulted in a 10-fold increase in affinity (Table 1). Thus, in contrast to upain-2, with mupain-1 we managed to achieve a considerable increase in affinity to the target enzyme by suitable substitutions.

The effects of substituting the same amino acid into the P1 position was in several cases strikingly different for upain-2 targeting human uPA as compared to mupain-1 targeting murine uPA. Substitution with L-homo-arginine (**6**) increased the affinity of upain-2 to human uPA but decreased the affinity of mupain-1 to murine uPA 5-fold; substitution with the Phe derivative **12** or the amidino compound **16**, respectively, decreased the affinity of upain-2 to human uPA, but increased the affinity of mupain-1 to murine uPA.

We confirmed the competitive nature of the inhibition with selected peptides, *i.e.*, **mupain-1-12** and **mupain-1-16**. The determined K_i values for inhibition of murine uPA, calculated with equation 2, were found to be indistinguishable at substrate concentrations ranging from 0.2 to 3 times the K_M value.

Importantly, the amidino compound **16**, L-homo-arginine (**6**) and the Phe derivative **12**, as free N-terminally acetylated and C-terminally amidated amino acids, were unable to inhibit human or murine uPA measurably in concentrations up to 400 μ M (data not shown).

Effects of P1 substitutions on the inhibition of chimeras between human and murine uPA by mupain-1 and upain-2. We considered two different hypotheses for the different effects of P1 substitutions on upain-2 inhibition of human uPA and on mupain-1 inhibition of murine uPA:

1. The different responses to the substitutions in human uPA on one side and murine uPA on the other could be due to the new amino acids in the P1 positions fitting differently into the S1 pockets of human and murine uPA, respectively.
2. The different responses to the P1 substitutions on inhibition of human and murine uPA could be related to the fact that the effect of a certain P1 substitution is strongly affected by the exosite interactions. As expected from the different sequences of the two peptides outside the P1 position and as demonstrated by site-directed mutagenesis and X-ray crystal structure determination (Andersen et al., 2008; Hansen et al., 2005; Zhao et al., 2007), the exosite interactions are very different for upain-2 and mupain-1. The exosite interactions may restrict the way the P1 residue inserts into the S1 pocket, and vice versa, thus determining how a certain P1 substitution affects the affinity.

To distinguish between these two possibilities, we constructed chimeras in which exosite and S1 pocket residues were exchanged between human and murine uPA. The choice of exosites was based on previous results from site-directed mutagenesis and X-ray crystal structure analysis (Figure 2). We previously demonstrated that “murinization” of human uPA in position 99, *i.e.*, generation of human uPA H99Y, made human uPA sensitive to inhibition by mupain-1, however, with a K_i value around 20-fold higher than the K_i value for inhibition of murine uPA (Andersen et al., 2008). We therefore used human uPA H99Y to study the importance of exosite interactions for mupain-1 binding. We also previously demonstrated an importance of the so-called 37 and 60 loops and of position 99 of human uPA for binding of upain-1 (Hansen et al., 2005; Zhao et al., 2007)(Figure 2). We now constructed and expressed a “humanized” murine uPA, with a human 37-loop (murine uPA Q35R, K36R, N37H, K37aR), a human 60-loop (murine uPA Q60aD, L60bY, N63D), and the human 99-residue grafted onto murine uPA (murine uPA Y99H). To evaluate the contribution from the S1 pocket, we constructed a human uPA variant which was murinized in position 192 (human uPA Q192K) and a variant of murine uPA which was humanized in position 192 (murine uPA K192Q). Position 192 is the only position with a non-conserved amino acid among the positions with residues lining the S1 pocket (Figure 2).

As a more radical way of exchanging residues, we constructed variants of murine uPA in which either the N-terminal β -barrel (residues 16 - 120) or the C-terminal β -barrel (residues 120 - 250) of the catalytic domain was replaced by the corresponding sequences of human uPA. All identified exosite interactions between upain-1 and human uPA involving non-conserved residues are present in the N-terminal β -barrel. Likewise, all identified exosite interactions between upain-1 and human uPA involving non-conserved residues are present in this β -barrel. In contrast, the S1 pocket is totally embedded in the C-terminal β -barrel (Figure 2).

We then tested the susceptibility of the constructed chimeras to the original upain-2 and mupain-1 peptides and to selected P1-substituted variants of upain-2 and mupain-1. The variants selected were variants with the amidino compound **16**, L-homo-arginine (**6**) or the Phe derivative **12** as

the P1 residue, because of the differential effect these substitutions have on the affinity of upain-2 to human uPA and of mupain-1 to murine uPA (Table 2).

Inspecting the data, it is seen that the susceptibility to upain-2 or mupain-1 is determined by the exosites, not position 192. In almost all cases, substitution with L-homo-arginine (**6**) either increased or left unchanged the affinity of upain-2 to the uPA variants, but decreased the affinity of mupain-1, while the reverse was true for substitutions with amino acids **12** and **16**. Strikingly, the latter P1 substitutions even resulted in a measurable affinity of mupain-1 to wt human uPA and human uPA Q192K, which were not measurably inhibited by the original mupain-1. Thus, the directions of the changes in affinities to the chimeras following substitutions of the P1 residues of upain-2 and mupain-1 were the same as those observed with wt human and murine uPA, although the fold changes were not exactly the same. In contrast, mutagenesis of position 192 did not change the direction of the changes. These results favour hypothesis 2 over hypothesis 1.

There were only a couple of exceptions to this generalization. Thus, substitution of the P1 residue of upain-2 with the amidino compound **16** (**upain-2-16**) unexpectedly resulted in a measurable inhibition of murine uPA, although the affinity remained low. Also, substitution of the P1 residue of mupain-1 with L-homo-arginine (**6**) (**mupain-1-6**) resulted in a slightly increased affinity to murine uPA with human 37 and 60 loops and position 99, while P1 substitution of upain-2 with L-homo-arginine (**6**) seemed to slightly decrease the affinity to the same uPA variant.

X-ray crystal structure analysis of a complex between a upain-2 variant and human uPA.
This analysis was followed by X-ray crystal structure analysis. However, we were restricted to analyze complexes between human uPA and upain-2 variants, as it has not yet been possible to crystallize complexes between mupain-1 and murine uPA. Among the complexes between human uPA and upain-2 variants, we were now able to determine the crystal structure of human uPA in complex with an upain-2 analog (**upain-2-13**) to a high resolution (1.32 Å) (Figure 4A). Peptide **upain-2-13** has a 10-fold lower affinity to human uPA than upain-2 (Table 1).

Structural analysis revealed that the uPA moiety of the uPA-**upain-2-13** complex has a conformation almost identical to that of uPA in complex with the original **upain-1** (Zhao et al., 2007) (rmsd of 0.35 Å). Further, the guanidino group of **13** forms five hydrogen bonds with uPA residues in

the S1 pocket. This hydrogen bonding scheme is similar, although not identical, to that of the P1 L-Arg in the complex between uPA and **upain-1** (Zhao et al., 2007) (Figure 3). In the uPA-**upain-2-13** complex, the guanidino group aligns well with the carboxyl group of Asp189, allowing the formation of two bifurcated hydrogen bonds between these structures. Also, in this complex, the N^c atom is hydrogen-bonded to Gly219 (Figure 3B). In the uPA-**upain-1** complex, only one of the Nⁿ's of the guanidino group hydrogen bonds with Asp189, while the other Nⁿ hydrogen bonds with Gly219. The contact surface areas in the S1 pocket in the **upain-1** complex and the uPA-**upain-2-13** complex are quite similar to each other (150 versus 154 Å²). Thus, the P1-S1 interaction in the uPA-**upain-2-13** complex is similar to that of the uPA-**upain-1** complex, however, the guanidino group in the uPA-**upain-2-13** complex probably has a more favourable hydrogen bonding pattern than in the uPA-**upain-1** complex.

In contrast to this conservation of P1-S1 interaction, the P3-P1' segments are quite different in the uPA-**upain-2-13** complex and uPA-**upain-1** complex. In the structure of uPA-**upain-2-13**, the peptide is moved toward the solvent and away from uPA by about 1.7 Å compared to **upain-1** (Figure 3C). As a result, **upain-2-13** has lost an intramolecular hydrogen bond (Trp3 to Ala6) which exists in **upain-1**. In addition, Trp3 in the uPA-**upain-2-13** complex makes less contact with uPA compared to the uPA-**upain-1** complex (64 versus 82 Å²), suggesting a potentially non-optimal interaction of the inhibitor with uPA. But the contacts between **upain-2-13** and the exosites in the N-terminal β-barrel remain unchanged. Thus, the anchoring of this peptide in the S1 pocket and to the N-terminal β-barrel exosites leads to a change of the P3-P1' segment and weakening of the interactions of Trp3 with uPA. This is in agreement with hypothesis 2.

Importantly, both the uPA-**upain-1** complex and the uPA-**upain-2-13** complex display decisive differences from the recently determined Michaelis complex between S195A uPA and its natural proteinaceous serpin inhibitor PAI-1 (Lin et al., 2011). In the uPA-PAI-1 Michaelis complex, the P2-P1' sequence inserts into the active site of uPA in a substrate-like fashion. Although the hydrogen bonding scheme of the P1 residue in the uPA-PAI-1 Michaelis complex is similar to that in the uPA-**upain-1** complex and the uPA-**upain-2-13** complex, the localisations of the P2 and P1'

residues are decisively different. The difference is caused by the inability of the bulky Trp residue in the P2 position of the inhibitory peptides to insert into uPA's S2 pocket (Figure 3B) and explains why upain-1 and upain-2-13 are unable to align into the active site in a substrate-like fashion, while PAI-1 is.

Discussion

We here report data elucidating the relative importance of active site and exosite interactions for the binding of peptidyl inhibitors to uPA. The data presented show that exosite interactions strongly influence the effect of a certain P1 substitution on the K_i values. From the data, it seems reasonable to conclude that there is a mutual dependence between the strength of the exosite interactions and the exact fit of the P1 residue into the S1 pocket, thus determining whether a certain P1 substitution affects the affinity positively or negatively. The determination of the K_i values was supplemented by X-ray crystal structure analysis of a upain-2 variant in complex with human uPA, demonstrating that the key to the effect of the P1 substitutions in upain-2 is the communication between the P1-S1 interactions and the interactions of upain-2's Trp3. Taken together, the data are in agreement with the above formulated hypothesis 2 rather than hypothesis 1.

Searching for quantitative patterns in the changes in K_i values following substitution of the P1 L-Arg with non-natural amino acids, we plotted the K_i values for inhibition of the various uPA variants by the various non-natural mupain-1 variants versus the corresponding values for the original mupain-1 in a double logarithmic plot (Figure 4). A similar plot could not be constructed for upain-2, as the K_i values were in too many cases above the level allowing an accurate determination. With the mupain-1 variants, we observed a linear relationship in such a plot (Figure 4). While there is no obvious molecular explanation for the linearity of the plot, it does allow us to draw an interesting inference about the effect of the substitutions. With both L-homo-arginine (**6**) and the Phe analog **12**, the slopes of the lines were less than 1 (0.62 and 0.66, respectively), indicating that P1 substitutions with these amino acids generally caused more increase or less decrease in affinity, the lower the affinity of original mupain-1 peptide to the target enzyme. But with the amidino compound **16**, the slope was 0.89, showing that the fold change in K_i was almost independent of the target. On the basis of this observation, one may suggest that the effect of the substitutions also partly depends on a target-independent element. This dependence cannot be explained by neither hypothesis 1 nor hypothesis 2, but may rather be related to a destabilisation of the unbound state of the peptide.

Comparison of the roles of murine and human uPA in xenografted tumors may help to delineate the relative importance of tumor and host uPA in tumor growth and spread. Availability of species-

specific inhibitors is therefore important. While a number of inhibitors of human uPA have been developed, the species specificity has been studied in only a few cases. Species specific inhibitory polyclonal and monoclonal antibodies (Blouse et al., 2009; Dano et al., 1980; Kaltoft et al., 1982; Lund et al., 2008; Petersen et al., 2001) are available but lack some of the advantageous properties of peptides. Some aryl-amidine-based, small molecule inhibitors had a strong preference (up to 203-fold) for human uPA over murine uPA (Klinghofer et al., 2001). While naphthamidine targeted only the S1 pocket and was equally potent with human and murine uPA, the specificity for human uPA increased with increasing number and increasing size of the side-chains. X-ray crystal structure analysis demonstrated that the most specific inhibitors interacted with Asp60a in human uPA, but no mutagenesis was performed to test this suggestion. Nevertheless, the observation is in agreement with our finding that specificity depends on exosite interactions (Figure 2) (Andersen et al., 2008; Hansen et al., 2005; Zhao et al., 2007).

The strong species specificities of upain-2 and mupain-1 depend on the interaction of the peptides with species specific surface loops outside the active site (Figure 2). Human or murine uPA can be made susceptible to mupain-1 or upain-2 by grafting mouse-specific residues onto human uPA or human-specific residues onto murine uPA (Table 2). In this context, one also notes that substitution of the P1 L-Arg residue with the amidino compound **16**, L-homo-arginine (**6**) or the Phe derivative **12** may deteriorate the species specificity. This could be due to a larger fraction of the binding energy depending on interactions within the S1 pocket or other target-independent contributions. Several examples illustrate this point. Thus, the original mupain-1 is a >2000-fold better inhibitor of murine uPA than of human uPA, but **mupain-1-12** is only a 300-fold better inhibitor of murine uPA than of human uPA. Nevertheless, **mupain-1-16**, the best mupain-1 variant developed until now, still displays an about 2000-fold selectivity for murine uPA over human uPA. This high specificity could indicate that **mupain-1-16** also will be specific among serine proteases in general, which combined with a favorable K_i (45 nM), makes **mupain-1-16** a candidate for use in *in vivo* experiments.

Authorship Contributions.

Participated in research design: Sørensen, K.J. Jensen, Hosseini, Andreasen.

Conducted experiments: Yuan, Sørensen, Hosseini, Jiang, Christensen, J.K. Jensen.

Contributed new reagents or analytic tools: Sørensen, Andersen, Hosseini, Fogh.

Performed data analysis: K.J. Jensen, Hosseini, Huang, Andreasen, Sørensen, Christensen, J.K. Jensen.

Wrote or contributed to the writing of the manuscript: K.J. Jensen, Hosseini, Huang, Andreasen, Sørensen, J.K. Jensen.

References

- Abramowitz N, Schechter I and Berger A (1967) On the size of the active site in proteases. II. Carboxypeptidase-A. *Biochem Biophys Res Commun* **29**(6):862-867.
- Andersen LM, Wind T, Hansen HD and Andreasen PA (2008) A cyclic peptidyl inhibitor of murine urokinase-type plasminogen activator: changing species specificity by substitution of a single residue. *Biochem J* **412**(3):447-457.
- Andreasen PA, Egelund R and Petersen HH (2000) The plasminogen activation system in tumor growth, invasion, and metastasis. *Cell Mol Life Sci* **57**(1):25-40.
- Blouse GE, Dupont DM, Schar CR, Jensen JK, Minor KH, Anagli JY, Gardsvoll H, Ploug M, Peterson CB and Andreasen PA (2009) Interactions of plasminogen activator inhibitor-1 with vitronectin involve an extensive binding surface and induce mutual conformational rearrangements. *Biochemistry* **48**(8):1723-1735.
- Boyar A and Marsh RE (1982) L-Canavanine, a Paradigm for the Structures of Substituted Guanidines. *J Am Chem Soc* **104**(7):1995-1998.
- Branden C and Tooze J (1991) *Introduction to protein structure*. Garland Pub., New York.
- Dano K, Nielsen LS, Moller V and Engelhart M (1980) Inhibition of a plasminogen activator from oncogenic virus-transformed mouse cells by rabbit antibodies against the enzyme. *Biochim Biophys Acta* **630**(1):146-151.
- DeLano (2002) The PyMOL Molecular Graphics System. *San Carlos, CA*.
- Dennis MS, Eigenbrot C, Skelton NJ, Ultsch MH, Santell L, Dwyer MA, O'Connell MP and Lazarus RA (2000) Peptide exosite inhibitors of factor VIIa as anticoagulants. *Nature* **404**(6777):465-470.
- Emsley P and Cowtan K (2004) Coot: model-building tools for molecular graphics. *Acta Crystallogr D Biol Crystallogr* **60**(Pt 12 Pt 1):2126-2132.
- Hajdin K, D'Alessandro V, Niggli FK, Schafer BW and Bernasconi M (2010) Furin targeted drug delivery for treatment of rhabdomyosarcoma in a mouse model. *PLoS One* **5**(5):e10445.
- Hansen M, Wind T, Blouse GE, Christensen A, Petersen HH, Kjelgaard S, Mathiasen L, Holtet TL and Andreasen PA (2005) A urokinase-type plasminogen activator-inhibiting cyclic peptide with an unusual P2 residue and an extended protease binding surface demonstrates new modalities for enzyme inhibition. *J Biol Chem* **280**(46):38424-38437.
- Hartung R, Hitzel-Zerrahn F, Mueller T and Pietsch J (2005) Process for the hydrogenation of alipharyl-substituted (hetero)aromatic compounds containing asymmetric carbon atoms using platinum/rhodium catalysts. , (0205954 USp ed), USA.
- Hedstrom L (2002) Serine protease mechanism and specificity. *Chem Rev* **102**(12):4501-4524.
- Heinis C, Rutherford T, Freund S and Winter G (2009) Phage-encoded combinatorial chemical libraries based on bicyclic peptides. *Nat Chem Biol* **5**(7):502-507.
- Hekim C, Leinonen J, Narvanen A, Koistinen H, Zhu L, Koivunen E, Vaisanen V and Stenman UH (2006) Novel peptide inhibitors of human kallikrein 2. *J Biol Chem* **281**(18):12555-12560.
- Jorgensen L and Nielsen HM (2009) *Delivery technologies for biopharmaceuticals peptides, proteins, nucleic acids and vaccines*. J. Wiley, Chichester.
- Kaltoft K, Nielsen LS, Zeuthen J and Dano K (1982) Monoclonal-Antibody That Specifically Inhibits a Human-Mr 52,000 Plasminogen-Activating Enzyme. *P Natl Acad Sci-Biol* **79**(12):3720-3723.

- Kayser KJ, Glenn MP, Sebti SM, Cheng JQ and Hamilton AD (2007) Modifications of the GSK3beta substrate sequence to produce substrate-mimetic inhibitors of Akt as potential anti-cancer therapeutics. *Bioorg Med Chem Lett* **17**(7):2068-2073.
- Klinghofer V, Stewart K, McGonigal T, Smith R, Sarthy A, Nienaber V, Butler C, Dorwin S, Richardson P, Weitzberg M, Wendt M, Rockway T, Zhao XM, Hulkower KI and Giranda VL (2001) Species specificity of amidine-based urokinase inhibitors. *Biochemistry* **40**(31):9125-9131.
- Kocsis A, Kekesi KA, Szasz R, Vegh BM, Balczer J, Dobo J, Zavodszky P, Gal P and Pal G (2010) Selective Inhibition of the Lectin Pathway of Complement with Phage Display Selected Peptides against Mannose-Binding Lectin-Associated Serine Protease (MASP)-1 and-2: Significant Contribution of MASP-1 to Lectin Pathway Activation. *J Immunol* **185**(7):4169-4178.
- Krook M, Lindbladh C, Eriksen JA and Mosbach K (1998) Selection of a cyclic nonapeptide inhibitor to alpha-chymotrypsin using a phage display peptide library. *Mol Divers* **3**(3):149-159.
- Lin Z, Jiang L, Yuan C, Jensen JK, Zhang X, Luo Z, Furie BC, Furie B, Andreasen PA and Huang M (2011) Structural basis for recognition of urokinase-type plasminogen activator by plasminogen activator inhibitor-1. *Journal of Biological Chemistry* **286**(9):7027-7032.
- Lund IK, Jogi A, Rono B, Rasch MG, Lund LR, Almholt K, Gardsvoll H, Behrendt N, Romer J and Hoyer-Hansen G (2008) Antibody-mediated targeting of the urokinase-type plasminogen activator proteolytic function neutralizes fibrinolysis in vivo. *J Biol Chem* **283**(47):32506-32515.
- Otwinowski Z and Minor W (1997) Processing of X-ray Diffraction Data Collected in Oscillation Mode. *Methods in Enzymology* **276**:307-326.
- Petersen HH, Hansen M, Schousboe SL and Andreasen PA (2001) Localization of epitopes for monoclonal antibodies to urokinase-type plasminogen activator - Relationship between epitope localization and effects of antibodies on molecular interactions of the enzyme. *Eur J Biochem* **268**(16):4430-4439.
- Project. CC (1994) The CCP4 suite: programs for protein crystallography. *Acta Crystallogr D Biol Crystallogr* **50**(Pt 5):760-763.
- Puente XS, Ordóñez, G.R., and López-Òtin (2008) *The cancer degradome : proteases and cancer biology*. Springer, New York, NY.
- Rao PN, Peterson DM, Acosta CK, Bahr ML and Kim HK (1991) Synthesis of Cis-4-Aminocyclohexyl-D-Alanine and Trans-4-Aminocyclohexyl-D-Alanine Derivatives and Determination of Their Stereochemistry. *Org Prep Proced Int* **23**(1):103-110.
- Rockway TW, Nienaber V and Giranda VL (2002) Inhibitors of the protease domain of urokinase-type plasminogen activator. *Curr Pharm Design* **8**(28):2541-2558.
- Sassatelli M, Debiton E, Aboab B, Prudhomme M and Moreau P (2006) Synthesis and antiproliferative activities of indolin-2-one derivatives bearing amino acid moieties. *Eur J Med Chem* **41**(6):709-716.
- Spraggon G, Phillips C, Nowak UK, Ponting CP, Saunders D, Dobson CM, Stuart DI and Jones EY (1995) The Crystal-Structure of the Catalytic Domain of Human Urokinase-Type Plasminogen-Activator. *Structure* **3**(7):681-691.
- Walker B and Lynas JF (2001) Strategies for the inhibition of serine proteases. *Cellular and Molecular Life Sciences* **58**(4):596-624.
- Wu P, Leinonen J, Koivunen E, Lankinen H and Stenman UH (2000) Identification of novel prostate-specific antigen-binding peptides modulating its enzyme activity. *Eur J Biochem* **267**(20):6212-6220.

- Wu P, Weisell J, Pakkala M, Perakyla M, Zhu L, Koistinen R, Koivunen E, Stenman UH, Narvanen A and Koistinen H (2010) Identification of novel peptide inhibitors for human trypsins. *Biol Chem* **391**(2-3):283-293.
- Zhao G, Yuan C, Wind T, Huang Z, Andreasen PA and Huang M (2007) Structural basis of specificity of a peptidyl urokinase inhibitor, upain-1. *J Struct Biol* **160**(1):1-10.

Footnotes

This work was supported by the National Natural Science Foundation of China [30811130467, 30973567, 30770429]; the Danish National Research Foundation [26-331-6]; the Lundbeck Foundation [R19-A2173]; the Danish Cancer Society [DP 07043, DP 08001]; the Danish Research Agency [272-06-0518]; the Novo Nordisk Foundation [R114-A11382].

¹P1, P2, P3, P4, etc. and P1', P2', P3', etc. are of the nomenclature of Schechter and Berger (Abramowitz et al., 1967) and denote those residues on the amino-terminal and carboxyl sides of the scissile bond (P1-P1'), respectively. The corresponding binding sites in the active sites of the enzymes are referred to as S1, S2, S3, S4, etc., and S'1, S'2, S'3, S'4.

²Amino acid numbering used in the text and figures refers to the standard chymotrypsinogen template numbering.

³Each of the amino acids tested as the P1 residue was given a number n between 1 and 19 (see Table 1). The corresponding variants of upain-2 and mupain-1 were named upain-2-n and mupain-1-n, respectively.

Legends for figures

Fig 1. Synthesis of novel arginine analogs for use as P1 residues in upain-2 and mupain-1.

Chemical synthesis of the protected forms of new Arg analogs **11**, **13**, **14**, and **15** as well as the protected form of the precursor for **17**. After incorporation of **17** into peptides, the alloc protection was removed and the liberated amine guanidylated on-resin. Similar chemistry was used for the construction of peptides containing homoarginine.

Fig 2. Residues in human or murine uPA, which were implicated in binding of upain-1 and mupain-1, respectively. A, Alignment of the catalytic domains of human and murine uPA.

The residue numbering indicated is by the chymotrypsin template numbering (Spraggon et al., 1995). The N-terminal β -barrel is highlighted in green and the C-terminal β -barrel in wheat. The residues in the sequence of human uPA which are highlighted in light green were implicated in upain-1 binding by site-directed mutagenesis (Hansen et al., 2005): Arg35, Arg36, Arg37a, Tyr40, Phe59, Asp60a, Tyr60b, Tyr64, Tyr94, His99, Tyr151, Trp186. The residues in the sequence of murine uPA which are highlighted in dark red were implicated in mupain-1 binding by site-directed mutagenesis (Andersen et al., 2008): Lys41, His57, Tyr99, Lys143, Asp189, Ser195. **B, Overview of the structure of the uPA-upain-1 complex.** uPA is depicted in surface mode and **upain-1** in sticks with CPK colors. The N-terminal β -barrel of uPA is colored green; the C-terminal β -barrel of uPA is colored wheat. N-terminal β -barrel exosite residues implicated in upain-1 binding by site directed mutagenesis are indicated by light green. The lining of the S1 specificity pocket is colored red. Gln192 is colored firebrick. The figure was constructed from PDB file 2NWN (Zhao et al., 2007).

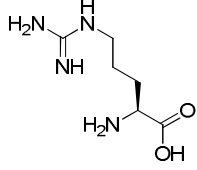
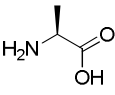
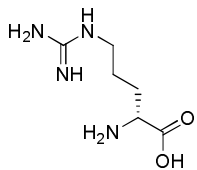
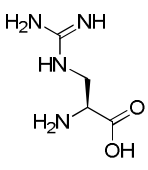
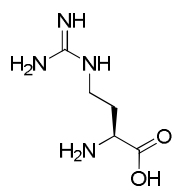
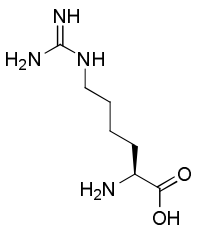
Fig 3. X-ray crystal structure analysis of the complex between human uPA and upain-2-13. A,

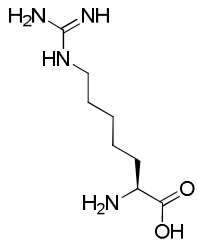
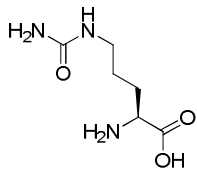
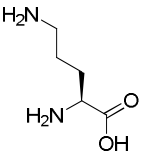
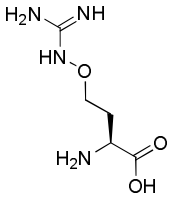
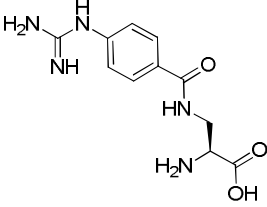
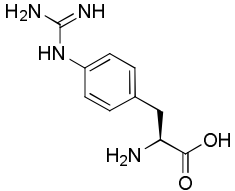
Overview of the complex between human uPA and upain-2-13. The uPA structure is shown as ribbons and **upain-2-13** is indicated in sticks with CPK colors. The electron density map (σ -weighted $2F_o - F_c$ omit map contoured at 1.0σ) of **upain-2-13** is shown in green. **B, Close-ups of the interactions of the P1 residues of various inhibitors within the S1 pocket of uPA.** The top panel shows the uPA-**upain-2-13** complex. The middle panel shows the uPA-**upain-1** complex (PDB file 2NWN (Zhao et

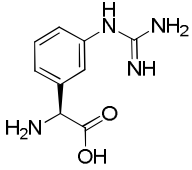
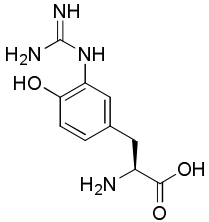
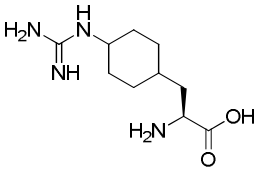
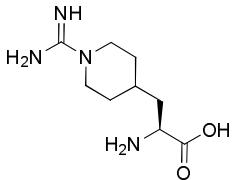
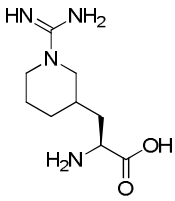
al., 2007)). The bottom panel shows the PAI-1-uPA Michaelis complex (PDB file 3PB1 (Lin et al., 2011)). Besides the P1 residues of the inhibitors, the figure also shows the P2 residues (Trp in **upain-2-13** and **upain-1** and Ala in PAI-1) and the P1' residues (Gly in **upain-2-13** and **upain-1** and Met in PAI-1) of the inhibitors and Asp189, Ser190, and Gly219 of uPA. **C, Comparison of the structures of upain-2-13 and upain-1 in their complexes with uPA.** The figure was constructed by aligning the uPA moieties of the complexes. **upain-2-13** is shown in sticks with CPK colors and **upain-1** in green.

Fig 4. The relationship between the K_i values for mupain-1 substituted with non-natural amino acids and the K_i values for mupain-1. The figure is based on the K_i values presented in Table 2 for wt human and murine uPA and human-murine uPA chimeras. Data points corresponding to K_i values above 500 μ M were omitted.

Table 1. K_i (μM) for inhibition of human uPA by upain-2 with P1 substitutions or inhibition of murine uPA by or mupain-1 variants with P1 substitutions

P1 residue	Chemical structure of P1 residue	upain-2 variants: K_i for inhibition of human uPA (μM)	mupain-1 variants: K_i for inhibition of murine uPA (μM)
L-arginine (1)		35 ± 8 (5)	0.55 ± 0.08 (8)
L-alanine (2)		$> 1000^{**}$	$> 1000^{***}$
D-arginine (3)		$> 1000^{**}$	$> 1000^{***}$
L-2,3-diaminopropionic acid-amidine (4)		$> 1000^{**}$	$> 1000^{***}$
L-nor-arginine (5)		$> 1000^{**}$	$> 1000^{***}$
L-homo-arginine (6)		23 ± 4 (3)*	2.88 ± 0.58 (5)***

L-bis-homo-arginine (7)		> 1000**	N.D. ¹
L-citrulline (8)		> 1000**	> 1000***
L-ornithine (9)		> 1000**	>500***
canavanine (10)		> 1000**	169 ± 9 (3)***
L-4-guanidino-benzoic acid- 2,3-diaminopropionic acid (11)		> 1000**	> 1000***
L-4-guanidino- phenylalanine (12)		> 500**	0.29 ± 0.02 (5)***

L-3-guanidino-phenylglycine (13)		316 ± 10 (3)**	343 ± 26 (3)** ²
L-3-guanidino-tyrosine (14)		> 1000 **	396 ± 35 (3)***
L-4-guanidino-cyclohexyl-alanine (15)		> 1000 **	0.92 ± 0.25 (3)***
L-3-(N-amidino-4-piperidyl)alanine (16)		> 1000 **	0.045 ± 0.010 (4)***
L-3-(N-amidino-3-piperidyl)alanine (17)		N.D. ¹	3.00 ± 0.34 (3)***

The K_i -values (μM) for the inhibition of S-2444 hydrolysis by human uPA by the indicated peptides were determined at 37°C. The table shows mean \pm standard deviation, with the number of determinations indicated in parentheses.

*Significantly different from the K_i values for inhibition of human uPA by **upain-2** ($p < 0.05$).

Significantly different from the K_i values for inhibition of human uPA by **upain-2 ($p < 0.005$).

***Significantly different from the K_i values for inhibition of murine uPA by **mupain-1** ($p < 0.005$).

¹Not determined

²Two peptides could be isolated with the same mass probably stemming from epimerization of the sensitive benzylic carbon. The other peptide had no measurable activity.

Table 2. K_i (μM) for inhibition of chimeras between human uPA and murine uPA by P1 substituted variants of mupain-1 and upain-2

P1 residue	Human wt	Human uPA H99Y	Human uPA Q192K	Human uPA H99Y-Q192K	Murine uPA Y99H, human 37 and 60 loops	Murine uPA K192Q	Murine uPA Y99H K192Q, human 37 and 60 loops	Murine uPA, human residues 16 - 120
L-arginine (1)	35 ± 8 (5) [*]	> 1000 ^{*,***}	77 ± 3 (3) ^{*,***,†}	>500 ^{*,***,†}	287 ± 124 (4) ^{*,***}	> 1000 ^{***}	351 ± 131 (3) ^{*,***,†}	19.3 ± 10.0 (5) ^{*,***,†}
L-homo-arginine (6)	23 ± 4 (3) [*]	>500 ^{*,***}	17.2 ± 0.8 (3) ^{*,***,†}	156 ± 56 (3) ^{*,**,**,†}	>500 ^{*,***}	432 ± 111 (3) ^{*,***,**}	313 ± 126 (3) ^{***,†}	12.9 ± 7.9 (3) ^{**,***,†}
-4-guanidino-phenylalanine (12)	>500 ^{*,**}	>500 [*]	>500	> 1000 [*]	>500 ^{*,**}	479 ± 190 (6) ^{*,**}	285 ± 83 (4) ^{***,†}	>500 ^{**}
3-(N-amidino-4-piperidyl)alanine (16)	> 1000 ^{*,**}	> 1000 ^{*,†}	> 500	> 1000 ^{*,**,*†}	> 1000 ^{**}	>500 [†]	> 1000 ^{**}	> 1000 ^{**†}
L-arginine (1)	> 1000	15.3 ± 2.0 (3) ^{***}	> 1000 [†]	9.4 ± 1.3 (3) ^{***,†}	21 ± 4 (4) ^{***,†}	1.27 ± 0.22 (4) ^{***,†}	36 ± 4 (3) ^{***,†}	499 ± 181 (4) ^{***,†}
L-homo-arginine (6)	> 1000	169 ± 17 (3) ^{*,***,†}	> 1000 ^{*,†}	72 ± 17 (3) ^{*,***,†}	14 ± 1 (4) ^{*,***,†}	11 ± 3 (3) ^{*,***,†}	66 ± 25 (3) ^{***,†}	285 ± 12 (3) ^{***,†}
-4-guanidino-phenylalanine (12)	93 ± 19 (3) [*]	1.86 ± 0.74 (3) ^{*,***,†}	54 ± 12 (3) ^{*,***,†}	1.71 ± 0.96 (3) ^{*,***,†}	1.2 ± 0.3 (3) ^{*,***,†}	0.35 ± 0.15 (3) ^{*,***}	1.25 ± 0.38 (3) ^{*,***,†}	34 ± 3 (3) ^{*,***,†}
3-(N-amidino-4-piperidyl)alanine (16)	93 ± 18 (4) ^{*,†}	2.48 ± 0.07 (3) ^{*,***,†}	74 ± 4 (3) ^{*,†}	1.04 ± 0.13 (3) ^{*,***,†}	1.1 ± 0.1 (3) ^{*,***,†}	0.24 ± 0.04 (3) ^{*,***,†}	2.40 ± 0.65 (3) ^{*,***,†}	31 ± 3 (3) ^{*,***,†}

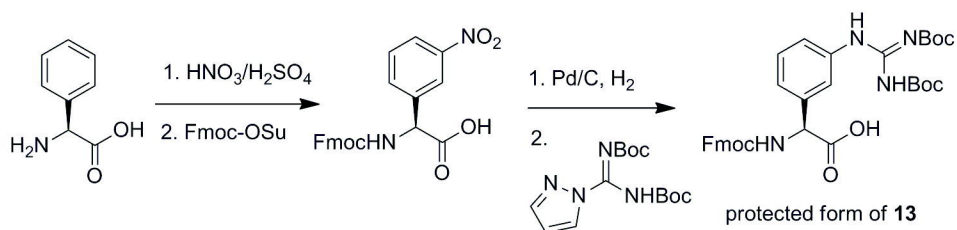
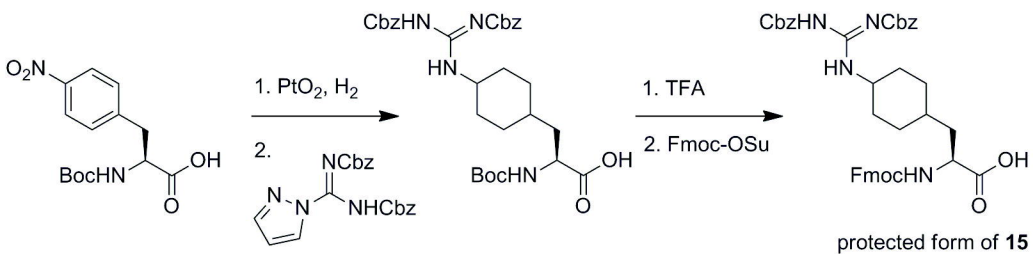
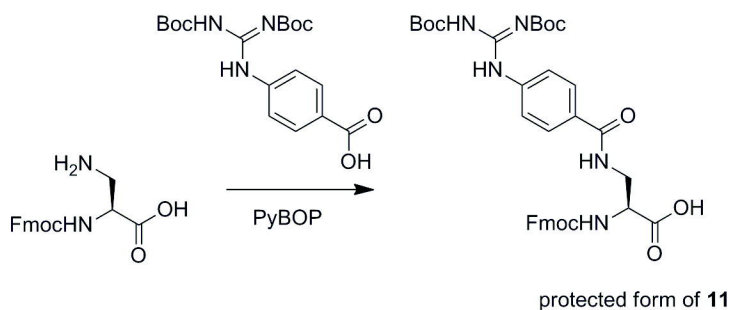
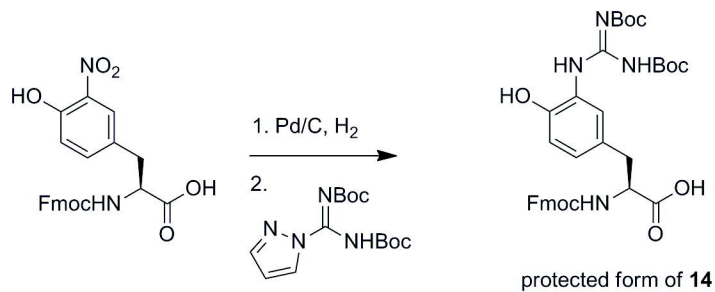
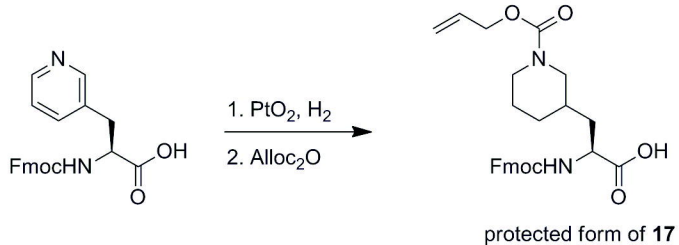
Murine uPA with human 37 and 60 loops have the mutations Q35R, K36R, N37H, K37aR, Q60aD, L60bY, N63D and Y99H. The K_i -values (μM) for the inhibition of S-2444 hydrolysis by human uPA or murine uPA by the indicated peptides were determined at 37°C. The table shows mean \pm standard deviation for the indicated number of determinations. Some data for the human and murine wt enzymes also shown in Table 1 are included to facilitate comparison.

*Significantly different from the K_i value for **mupain-1** ($p < 0.01$).

Significantly different from the K_i values for **upain-2 ($p < 0.01$).

***Significantly different from the K_i values for human wt uPA ($p < 0.01$).

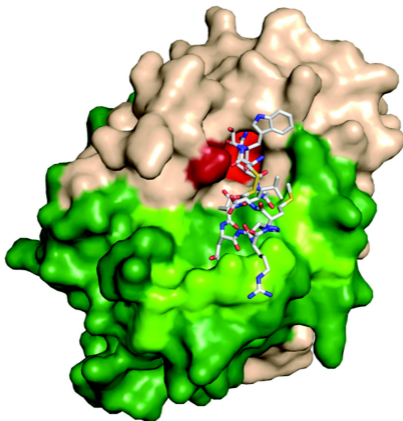
†Significantly different from the K_i values for murine wt uPA ($p < 0.01$)



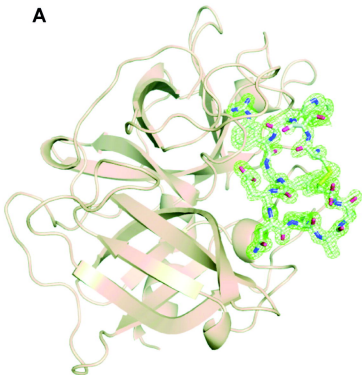
A

Human	1-	CGQKTLRPRF	KIIGGEFTTI	ENQPWFAAIY	RFHRGGSVTY	-VCGGSLMSP	CWVISAT ^H CF
Mouse	1-	CGQKALRPRF	KIVGGEFTEV	ENQPWFAAIY	QKNKGGSPPS	FKCGGSLISP	CWVASAA ^H CF
Human	60-	IDYPKKEDI	VYLGRSRLN-	SNTQGEMKFE	VENLILHKDY	SADTLA ^H HND	IALLKIRSKE
Mouse	60-	IQLPKKENYV	VYLGQSKESS	YNP-GEMKFE	VEQLILHEYY	REDSLAY ^H HND	IALLKIRTST
Human	110-	GRCAQPSRTI	QTICLPSMYN	D-PQFGTSCE	ITGFGKENST	DYL ^H PEQLKM	TVVKLISHRE
Mouse	110-	GQCAQPSRSI	QTICLPPRFT	DAP-FGSDCE	ITGFG ^H ESES	DYLYPKNLKM	SVVKLVSHEQ
Human	168-	CQQPHYYGSE	VTTKMLCAAD	PQ ^H KTDSCQG	DSGGPLVCSL	QGRMTLTGIV	SWGRGCALKD
Mouse	168-	CMQPHYYGSE	INYNMLCAAD	PEWKT ^H DSCGK	D ^H GGPLICNI	EGRPTLSGIV	SWGRGCAEKN
Human	224-	KPGVYTRVSH	FLPWIRSHTK	EENGLAL			
Mouse	224-	KPGVYTRVSH	FLDWIQSHIG	EEKGLAF			

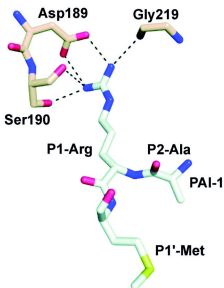
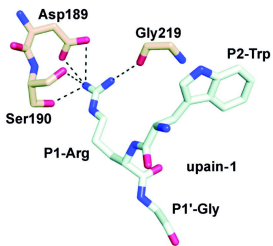
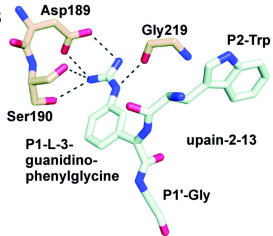
B



A



B



C

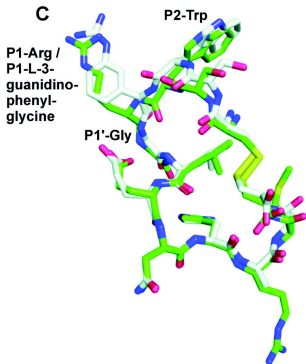
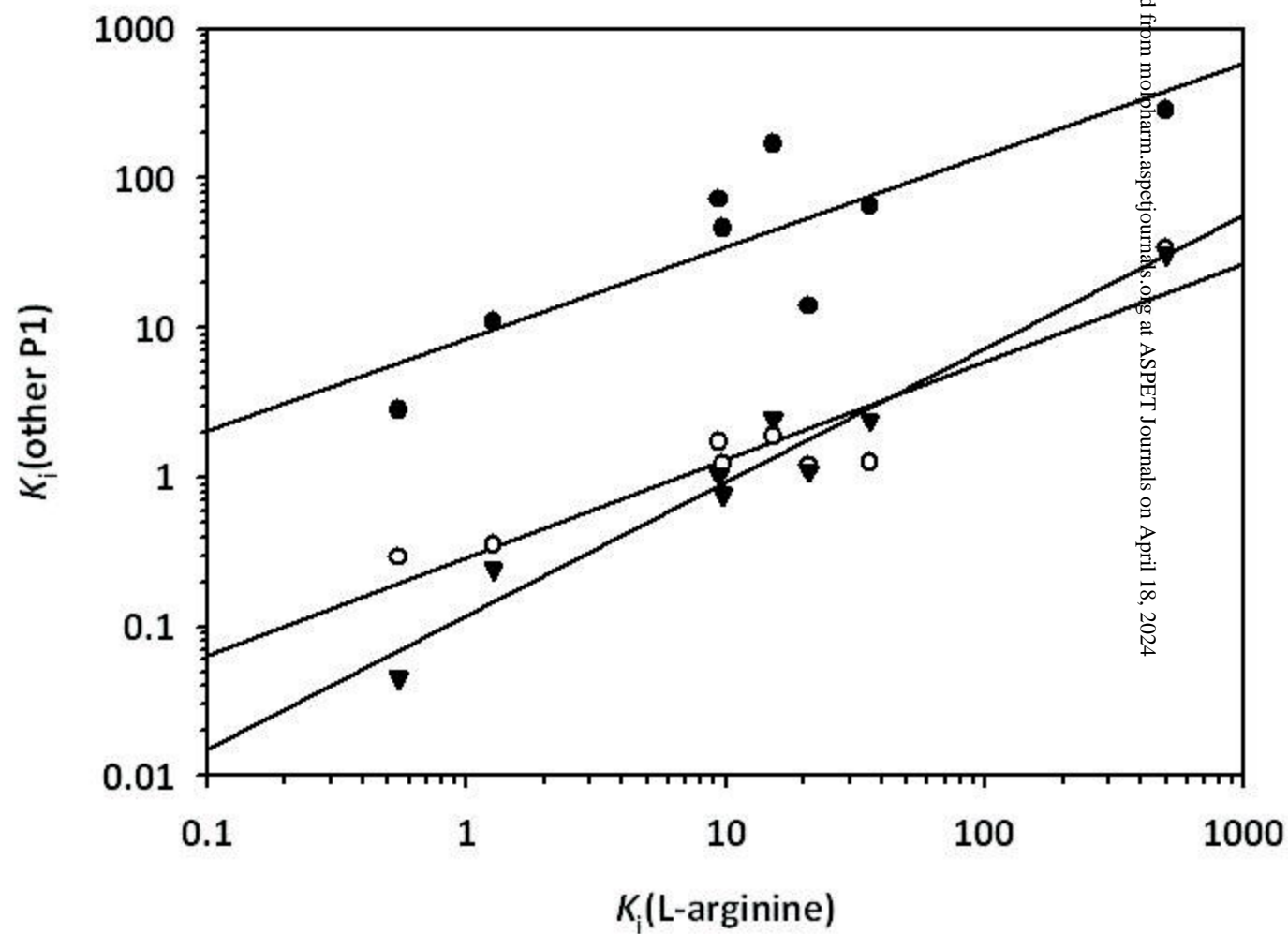


Figure 4



Downloaded from molpharm.aspetjournals.org at ASPET Journals on April 18, 2024

